Palaeogeography, Palaeoclimatology, Palaeoecology 625 (2023) 111691

Contents lists available at ScienceDirect

Palaeogeography, Palaeoclimatology, Palaeoecology

journal homepage: www.elsevier.com/locate/palaeo

Swimming and feeding in the Ordovician trilobite *Microparia speciosa* shed light on the early history of nektonic life habits

Jorge Esteve [a,*], Matheo López-Pachón [b]

[a] Departamento de Geodinámica, Estratigrafía y Paleontología, Facultad de CC. Geológicas, Universidad Complutense de Madrid, Spain
[b] Departamento de Ingeniería Mecánica, Universitat Rovira i Virgili, Tarragona, Spain

ARTICLE INFO

Editor: Prof. S Shen

Keywords:
GOBE
Arthropods
Nektonization
Computational fluid dynamics
Biomechanics

ABSTRACT

Computational Fluid Dynamic simulations (CFD) show that the Ordovician trilobite *Microparia speciosa* had a high stability in the horizontal plane (parallel to the flow currents), suggesting that it could be very stable in the water column when it was enrolled, for hovering or to get stabilization when the current disturbed the swimming. This indicates a new way to use enrolment in trilobites during the Ordovician radiation, not only for protection against predators or the environment but also as a hydrodynamic tool to maintain stability within the water column. Metachronal propulsion was likely used by *Microparia speciosa* for swimming and, in a high-viscosity scenario, also for feeding. This is suggesting given that the vortex below *Microparia speciosa* takes particles directly to the mouth, and taken more particles when the trilobite is orientated in the way of the current (and no countercurrent). This suggests a passive feeding strategy for better energy saving when the trilobite is hovering in water column.

1. Introduction

An understanding of how animals move is essential to proper contextualization of their evolutionary history and ecological impact. Eco-morphological differentiation between benthic and pelagic trilobites was already established in the aftermath of the Cambrian Explosion and some poorly streamlined Cambrian genera already show modifications in the trunk appropriate for a nektonic lifestyle (Fortey, 1985). However, during the Ordovician radiations, especially the Great Ordovician Biodiversification Event (GOBE), around 470–460 million years ago, many morphological novelties appeared, indicating that further and different ecological niches were gradually colonized (Shiino et al., 2014; Esteve et al., 2018; Stigall et al., 2019; Harper et al., 2020, 2021; Servais et al., 2023). Trilobites are evidently an important fossil group for studying the evolutionary processes and ecological pressures underlying early animal diversification events (Hopkins, 2014; Stigall et al., 2019). Although, it seems fair to assume that Cambrian or Ordovician trilobites were adapted for their environments, we are far from understanding the mechanics of their morphological designs and how they evolved as nektonic habits became more widespread in Palaeozoic seas.

Streamlined trilobites were likely good swimmers; this is the case in the Ordovician trilobite *Microparia,* the subject of the present study. But unlike recent pelagic or mesopelagic animals, the species *Microparia speciosa* Hawle and Corda, 1847 kept the ability to fully enroll (Marek, 1961, p. 38, pl. III, fig. 10, pl. IV, fig. 14). Enrolment was a helpful adaptive behavior to protect the body of benthic trilobites against predators and environmental disturbance (Esteve et al., 2011, 2012; Lerosey-Aubril and Angiolini, 2009; Ortega-Hernández et al., 2013). Although enrollment is relatively common in different *Microparia* species including *M. pratli* and *M. speciosa* (see Marek, 1961, pp. 38, 41), it seems less likely that enrolment was useful against predators in the water column because large pelagic predator could catch them anyway so faster escape may be considered more effective. We may then ask what was the reason for enrolment in a pelagic trilobite? Living arthropods show a high variation in morphological adaptations for swimming: from long antennae suitable to break surface-tension of the water and improve swimming in spiny lobsters (Jeffs and Holland, 2000) to a narrow ridge crest adapted to maintain orientation during fast swimming in small calanoid copepods (Lewis et al., 2006). But only partial enrolment has been observed in tiny planktic crustaceans, with fuller enrolment in the early developmental stages of some crustaceans (Dittrich, 1987; Haug and Haug, 2014). On the other hand, swimming and associated hydrodynamics always played an essential role for feeding in planktonic arthropods. Flow patterns assisted feeding (Koehl

* Corresponding author at: Departamento de Geodinámica, Estratigrafía y Paleontología, Facultad de CC. Geológicas, Universidad Complutense de Madrid, Spain.
E-mail address: jorgeves@ucm.es (J. Esteve).

https://doi.org/10.1016/j.palaeo.2023.111691
Received 16 November 2022; Received in revised form 22 May 2023; Accepted 15 June 2023
Available online 20 June 2023

and Strickler, 1981; Marshall, 1973; Strickler, 1982) in pelagic and mesopelagic arthropods with filter and suspensory feeding habits (Lowndes, 1935; Paffenhöfer et al., 1982). However, despite the anatomical evidence in pelagic trilobites, which suggests filter-feeding habits or direct planktonic feeders (Fortey and Owens, 1999), we have no insights into the feeding mechanisms of early pelagic animals. In this work, we explore the hydrodynamics of *Microparia speciosa*, in order to understand nektonic adaptations for swimming and feeding, using computational fluid dynamic simulations (CFD) to assess plausible scenarios for feeding in an ancient pelagic habitat.

2. Material and methods

A three-dimensional digital reconstruction of *Microparia speciosa* (L16649), based on an x-ray microtomography scan of a beautiful 3D internal mould of an enrolled specimen from the Šárka Formation (middle Ordovician, Czech Republic) and housed at the National Museum of Prague, was used in the CFD analyses (See Data S1 in the supplementary data). Seventy-five simulations of water flow around the *Microparia speciosa* reconstruction were performed using OpenFOAM V.6. Following (Esteve et al., 2021) procedure, summarized here. The simulations were conducted with *Microparia speciosa* at five different orientations to the current (0°, 45°, 90, 135°, and 180°) in both prone and enrolled position, using a range of flow velocities (0.007 m/s to 2.5 m/s) that embrace the typical velocities for open oceanic settings on the continental shelf (Lumpkin and Johnson, 2013), and which also reflect a pelagic or mesopelagic environments (Fig. 1A-C, Table 1). We could not model limbs because legs were not part of the model because they are unknown in the fossil state, and meshing and modelling them would have been extremely difficult and time-consuming. Three computational domains with subsequent refinement boxes around model *Microparia speciosa* were defined to carry out the simulations for both prone and enrolled models and to more accurately simulate flow in the wake and downstream of the model (Fig. 2D-H). Prism layers were generated along the model surface to simulate the viscous effects of the boundary

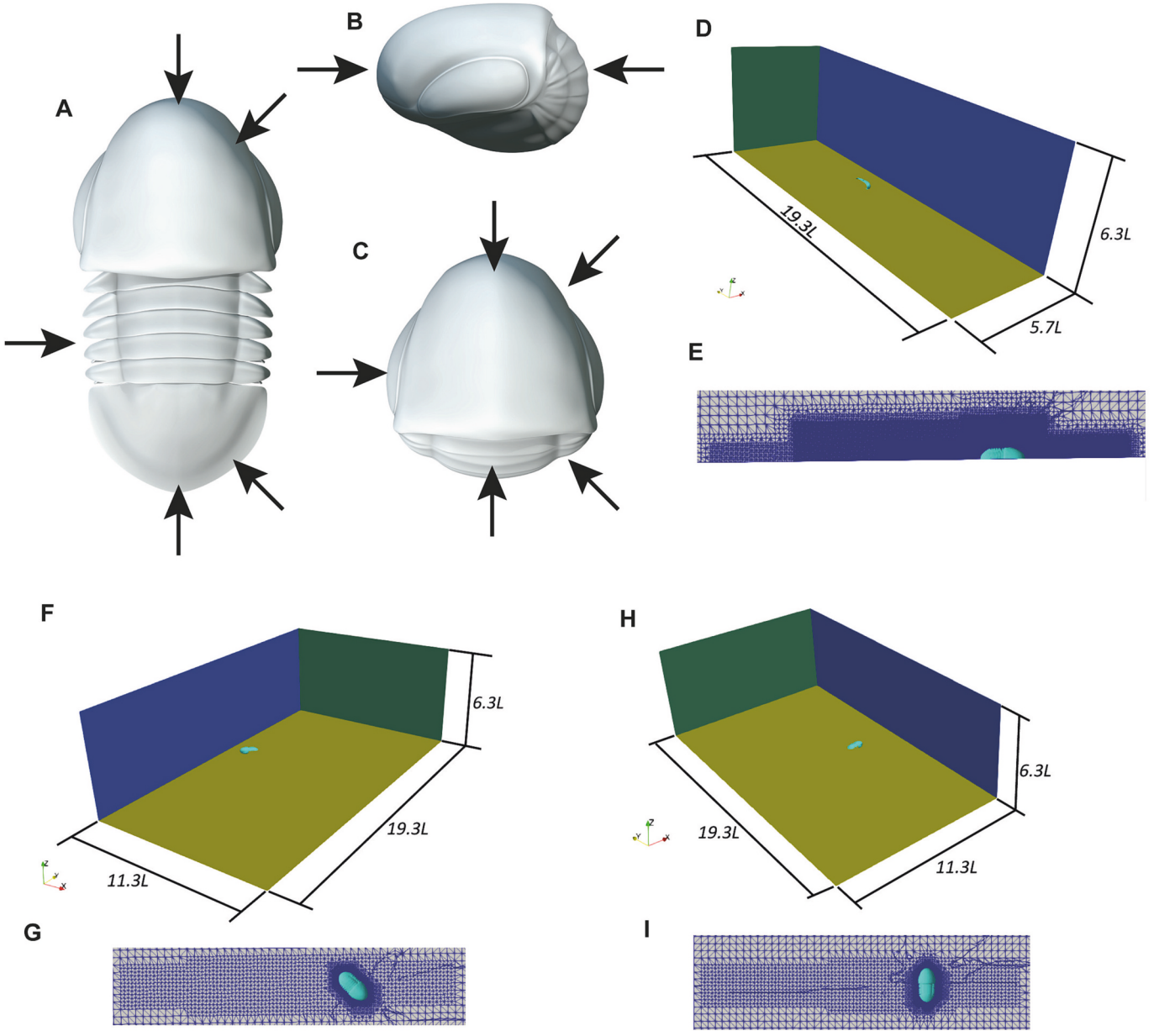

Fig. 1. A-C 3-D Model of *Microparia speciosa*, arrows point out the flow directions. A. Prone models B-C. Enrolled model. D-H. Computational domain for simulations with D-E frontal and read flows; F-G obliques flows and H-I. Cross flow.

layer; for the majority of the surface, five layers were made to obtain a y^+ value less than 1 for the whole model. The meshing results were highly acceptable since the quality criteria were in the standard range. The optimal mesh size was determined by carrying out a sensitivity analysis with meshes ranging from ~2,400,000–5,000,000 elements in size. The inferred properties of Ordovician seawater (Esteve et al., 2021; Lumpkin and Johnson, 2013; Veizer et al., 1997; Veizer and Prokoph, 2015) were used in the simulation; the fluid was treated as isothermal, incompressible, and Newtonian, with environmental conditions deduced for the Ordovician informing the physical properties of the fluid (Table 2). Given that *Microparia speciosa* is interpreted as a mesopelagic arthropod (Fortey, 1985; Fortey and Owens, 1999) the lower surface (seafloor) is far enough to interfere its hydrodynamics. However, a moving wall condition with the inlet velocity was applied to the ground. Finally, the outlet had a pressure condition equal to the barometric pressure. The Reynolds number (eq. 1) is the relation of viscous forces to inertial forces within a fluid subjected to relative internal movement due to different fluid velocities.

$$\Re = \frac{\rho V L}{\mu} \tag{1}$$

Where the density of the fluid is ρ, V is the freestream velocity, L is the characteristic length and, μ is the kinematic viscosity of the fluid. The Reynolds number determines whether a flow is in a turbulent or

Table 1
Velocities for open oceanic settings on the continental shelf and Reynolds number (*Re*).

Enrolled		Prone	
V [m/s]	***Re***	**V [m/s]**	***Re***
0.007	213.15	0.03	503.56
0.1	3044.97	0.1	1678.52
0.25	7612.42	0.5	8392.60
0.35	10,657.39	1	16,785.20
0.5	15,224.84	1.5	25,177.80
1	30,449.68	2.5	41,963.00
1.5	4.567.452.431		
2.5	7.612.420.719		

Table 2
Properties of the working fluid.

Sea Properties	
Temperature (°C)	26
Density (kg/m^3)	1055.1
Max Reynolds	1.17×10^4
Dynamic viscosity (kg/m s)	9.98×10^4
Salinity (ups)	35

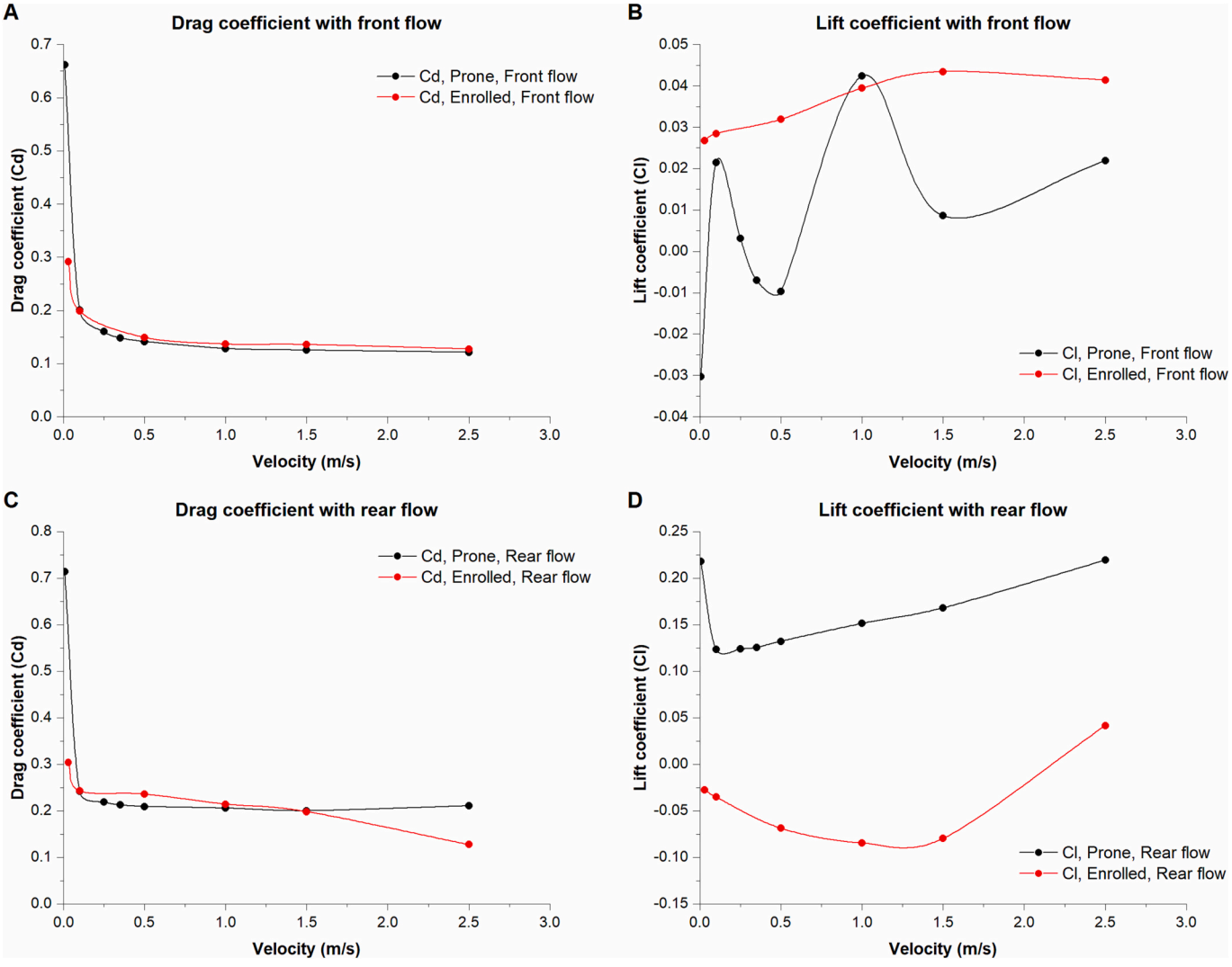

Fig. 2. Drag and lift coefficients.

laminar regime. Given the Reynolds number, between 213.15 and 7,612,420,719 (Table 1), and because this work aims to assess hydrodynamics in stable environmental conditions, we performed the analysis under laminar flow conditions. A pressure-based solver, SIMPLE (Semi-Implicit Method for Pressure-Linked Equations), was used as a pressure-velocity coupling for the steady simulations.

3. Results

3.1. Drag and lift coefficients

The drag coefficient is a dimensionless number that is used to quantify the resistance force of an object immersed in a fluid. In the case of a moving ground vehicle, for example, the fluid would be the atmospheric air flowing around the vehicle. The drag forces are due to "pressure" and "friction" effects. The drag coefficient is defined mathematically as (eq. 2):

$$C_d = \frac{2F_d}{\rho V^2 A} \quad (2)$$

where Fd corresponds to the drag force, ρ is fluid density, V is the freestream velocity, and A is the cross-sectional area. On the other hand, the lift coefficient is a dimensionless number that is used to understand the vertical forces of the fluid around the object geometry. This parameter describes the relative pressure from the fluid-generated forces in the whole surface of the object geometry in a flow field. The lift coefficient is defined mathematically as (eq. 3):

$$C_L = \frac{L}{\frac{1}{2}\rho V^2 A} \quad (3)$$

where L is the lift force, ρ is the fluid density, V is the freestream velocity, and A is the cross-sectional area.

The drag coefficient (C_D) when the flow is coming from the front which generally decreases as velocity increases, becoming almost constant after 0.5 m/s ($C_d \approx 0.10$) in both simulations, prone and enrolled (Fig. 2A). When the trilobite is enrolled the C_D is lower than the prone simulation in velocities close to 0. The lift coefficients (C_L) in simulations with the flow from the front are around 0 in both configurations, with an unstable pattern in the prone simulation fluctuating between −0.04 and + 0.004 and more stable in the enrolled position around 0.03 (Fig. 2B). The drag coefficient shows the same pattern when the flow is coming from the rear part (Fig. 2C) and even decreases in higher velocities (above 1.5 m/s) in the enrolled simulation. When the flow is coming from the rear part the C_L in the enrolled simulation shows very low negative coefficients between −0.05 and 0.025 (Fig. 2D). In this case the prone simulation is slightly more stable ($C_L \approx 0.10$) also with low velocities and increasing in higher velocities (Fig. 2D). Simulations with cross flows shows also very low drag coefficient in the prone ($C_D \sim 0.6$) and enrolled ($C_D \sim 0.4$) models, while for cross flows the simulations shed negative values for the lift coefficients (Fig. 3). The drag coefficient with the front flow at 45° shows very low values for the prone position ($C_D \sim 0.5$), slightly lower in the enrolled position ($C_D \sim 0.4$) (Fig. 4A). The lift coefficients (C_L) in simulations with the flow from the front and rear at 45° display values around 0 in the enrolled models, even slightly negative values in the simulation with rear flow (Fig. 4C-D). When the flow is coming from the rear the model in enrolled position shows the same pattern while in the prone position the drag coefficient increases around 0.9 (Fig. 2D). The simulations using the prone models show higher drag coefficient compare with those enrolled simulations with oblique flow.

3.2. Velocity fields

The results show that flow velocity decreases rapidly where it first encounters the *Microparia speciosa* reconstruction, with a steep velocity gradient (the boundary layer) developing as the flow approaches the lower and upper margins of the simulation volume. When the flow is coming from the front, the field velocities show a vortex under the body of *Microparia speciosa* and an elongate low velocity flow region (the wake) form downstream of the trilobite in prone and enrolled positions (Fig. 5A-C, 6A-D). The wake in the prone simulations is rather symmetrical in lower and higher velocities. But the wake shows two vortices in the enrolled simulation (closer to the trilobite body at higher flow velocities, see in Fig. 6B) with a very asymmetric geometry in higher velocities, pushing up the trilobite in the water column (Fig. 6A-D). When the flow is coming from the rear the wake is formed also downstream of the trilobites, in the case in front of its head (Fig. 5D). However, the wake shows asymmetric geometry in the simulation of the prone *Microparia speciosa* with a vortex in the lower part of the wake (Fig. 5E). This vortex reduces its size and happens close to the anterior part of the head with higher velocities and pushes up the trilobite increasing the lift (Fig. 5F). The vortices seen in all wakes approaches the trilobite body with higher velocity of the flow. It is interesting to point out that the developed vortex below the *Microparia speciosa* body could drive particles directly to the hypostome where the mouth was situated (Fig. 5A, B, D. See movies S1-S6 in the supplementary material). In addition, the transverse hypostome in *Microparia speciosa* permits the

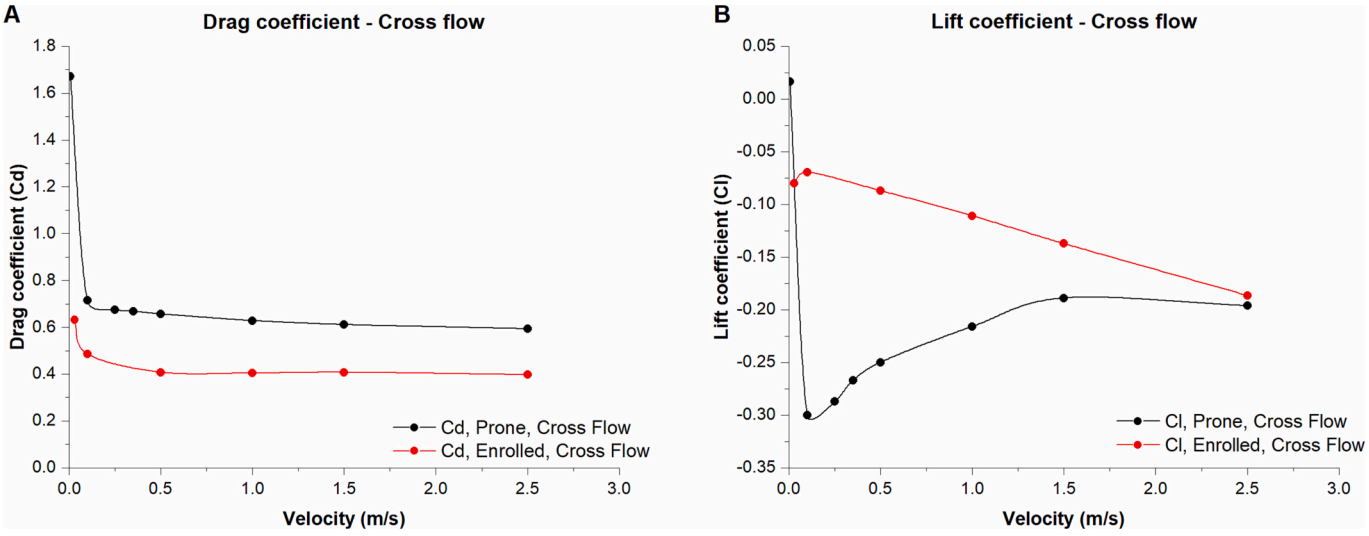

Fig. 3. Drag and lift coefficients.

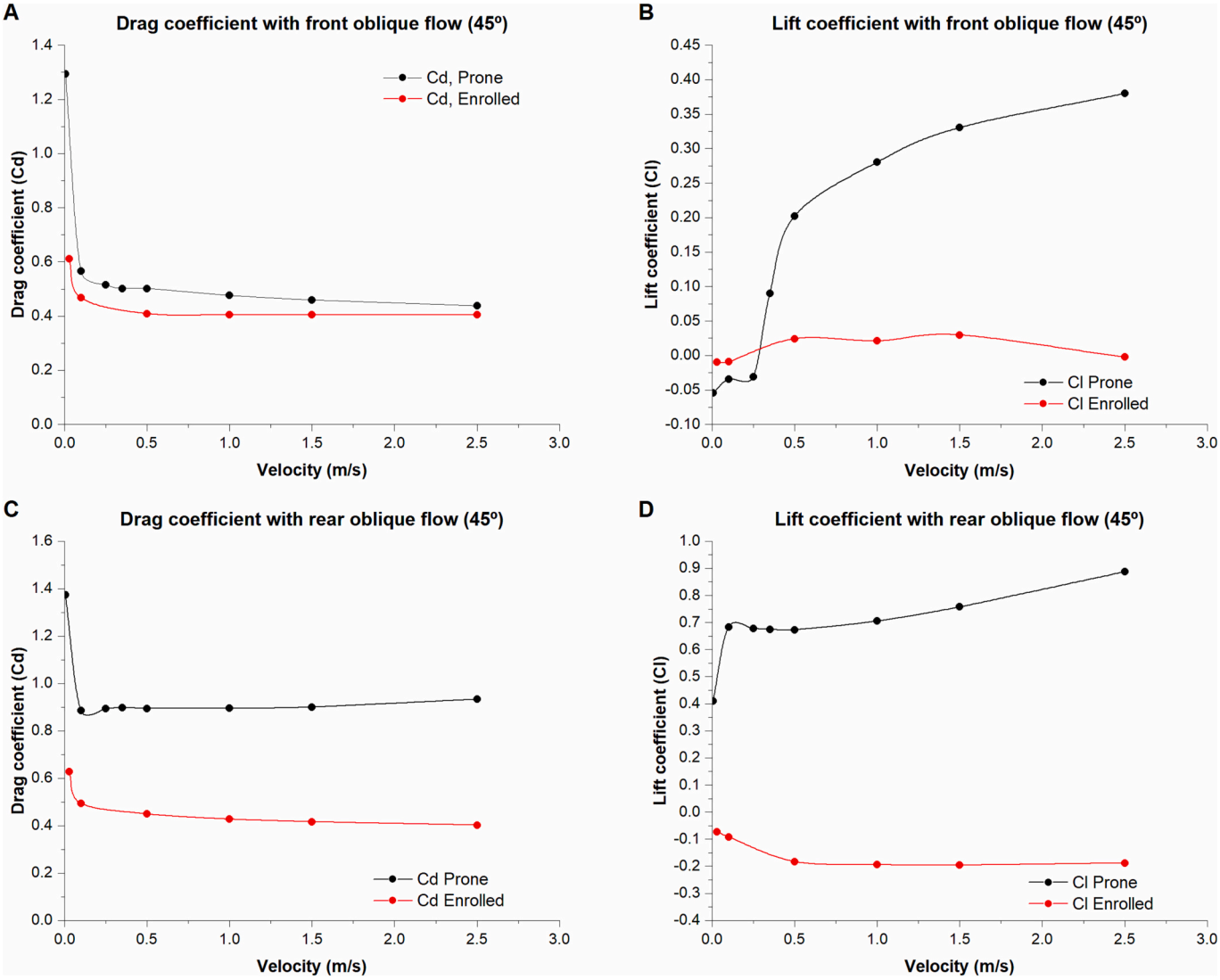

Fig. 4. Drag and lift coefficients.

lateral low flows to converge below the hypostome (See movies S1-S2 in the supplementary material). The large vortex below the body is closer to the body when the flow is coming from the rear part (Fig. 5D, see movies S1-S2 in the supplementary material). Also, while particles in the anterior part of the vortex decrease rapidly the velocity those particles in the rear part of the vortex increase the velocity (see video S1 in the supplementary material).

Transversal and oblique (45° front and rear) flows generate a very irregular wakes rather symmetrical to the current but without ventral vortex in prone (Fig. 5G-L) and enrolled simulations (Fig. 6K-O). The wake in the transversal flow generates two vortexes in the anterior part of the trilobite body (see arrows in Fig. 5H). Oblique flows from the anterior and rear part generate similar irregular wake pattern (Fig. 5K, L).

3.3. Preassure coeffient

The pressure coefficient (C_p) is a non-dimensional number, which explains the relationship between static and dynamic pressure in a surface, eq. (4).

$$C_p = \frac{p - p_\infty}{\frac{1}{2}\rho V_\infty^2} \quad (4)$$

Where p is the static pressure in the point of interest; p_∞ is the static pressure in the freestream; ρ is the freestream fluid density and V_∞ is the freestream velocity of the fluid. In this specific case, the exoskeleton of *Microparia speciosa* provides the geometry. Stagnation points were recognized when the C_p values approached 1. For the *Microparia speciosa* models tested, flow velocity was low in the rear part with front flows and in the anterior part with rear flows, where the lowest pressures were concentrated in the dorsal exoskeleton (Fig. 7A-B). The cephalic doublure shows negative pressures when the flow is coming from both, anterior and posterior part (Fig. 7C-D), close to a neutral pressure when the flow is coming from the posterior part (Fig. 7D). The dorsal exoskeleton with frontal flows displays negative pressures and values near zero in the last three segments and the pygidium as well as in the ventral side (Fig. 7A, C), only lateral sides of the cephalic doublure show positive values counteracting the higher (negative) values displayed in the rostral plate and the hypostome (Fig. 7C-D). When the flow is coming from the rear part higher pressures are displayed in the posterior part of the occipital ring and anterior part of the first thoracic segment (Fig. 7B). In the simulations with the enrolled configurations show similar patterns. Highest pressures are concentrated where the flow encounters, the snout when the flow is coming from the anterior part and the second, third and fourth segments when the flow is coming from the posterior part (Fig. 7E-H). Higher pressures are observed in the

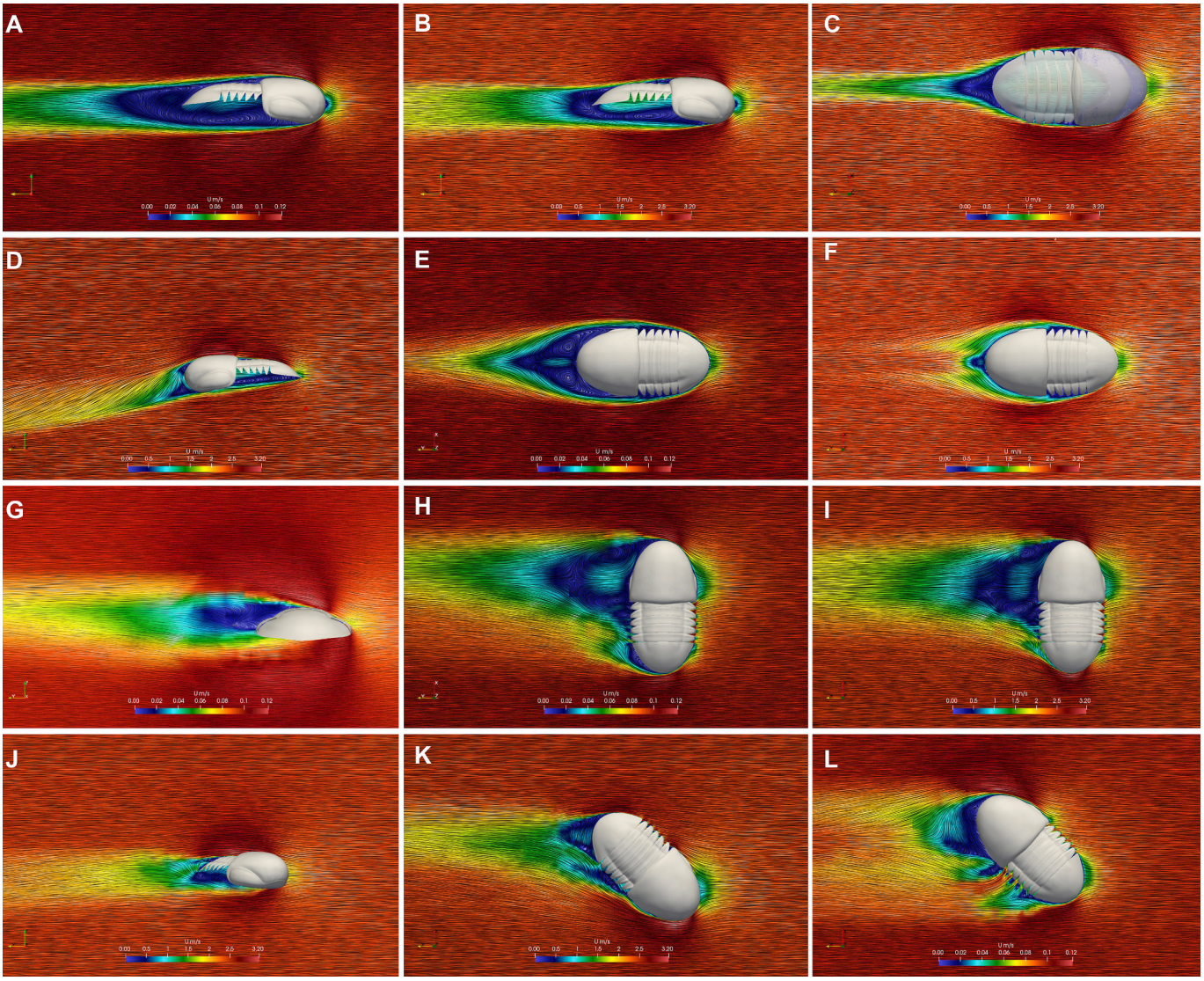

Fig. 5. Velocity field for CFD simulations in prone position.

simulations where the flow encounters *Microparia speciosa* for all simulations. As a consequence, as the flow velocity increased, the stagnation area decreased. However, the C_p values were higher in magnitude, for instance they had more intense red color in 0.25 m/s in for the higher pressure. These phenomena also increased the lift coefficient due to a lifting force applied to the *Microparia speciosa* body (Figs. 2D, 3B, 4B, D). However, in the simulations with the enrolled models the higher pressures do not increase with higher flow velocities, consequently the lift coefficient does not increase or even decreases (Figs. 3B, 4B, D) except for simulations with the flow from the rear part.

4. Discussion and conclusions

4.1. Swimming

Arthropods mainly use three different propulsive mechanisms for swimming: i) oar strokes or drag-based paddling ii) propeller thrust and iii) rotary beats (Lochhead, 1961, 1977,). But despite of the lack of appendages in our analysis and given that the main components we use to investigate swimming are the drag, lift and pressure coefficients (Hessler, 1985; Jacklyn and Ritz, 1986; Strickler, 1977), we can identify the mechanisms for swimming in *Microparia*. The results of our study clearly indicate that there are significant differences both in the drag and lift coefficients for prone and enrolled models.

The drag coefficient is useful for comparing the hydrodynamics among swimming animals (Colin et al., 2020). The drag coefficient of the nektobentonik trilobite *Hypodicranotus striatus* ranges from 1.5 and 0.5, between 0 and 0.5 m/s (Shiino et al., 2012, 2014) while in the benthic trilobite *Placoparia cambriensis* ranges from 0.8 and 0.4, between 0 and 0.5 m/s (Esteve et al., 2021). *Microparia speciosa* shows lower drag coefficient in the same ranges of current velocities (here we tested between 0 and 2.5 m/s) keeping below 0.2 under the same conditions by Shiino et al. (2012, 2014) and Esteve et al. (2021). According to these previous works and our results we can predict that for small swimmers at low velocities viscous forces are more important than inertial forces in determining drag. This means that streamlining may be less important for small or slow animals and explains the low drag coefficient measured in *P. cambriensis* and *H. striatus*. *Microparia speciosa* was a small and well streamlined trilobite, but besides low drag coefficient propulsions of swimming were necessary if *Microparia speciosa* swam effectively. When *Microparia speciosa* was swimming with a favorable current, the relative low-pressure regions generated in the fluid surrounding the exoskeleton of *Microparia*, which are observed by using particle paths in the flow velocity fields (Fig. 5D, see movies S1-S6 in the supplementary material) and the pressure coefficient suggests that, rather than pushing against the surrounding fluid, *Microparia speciosa* primarily pulled itself through

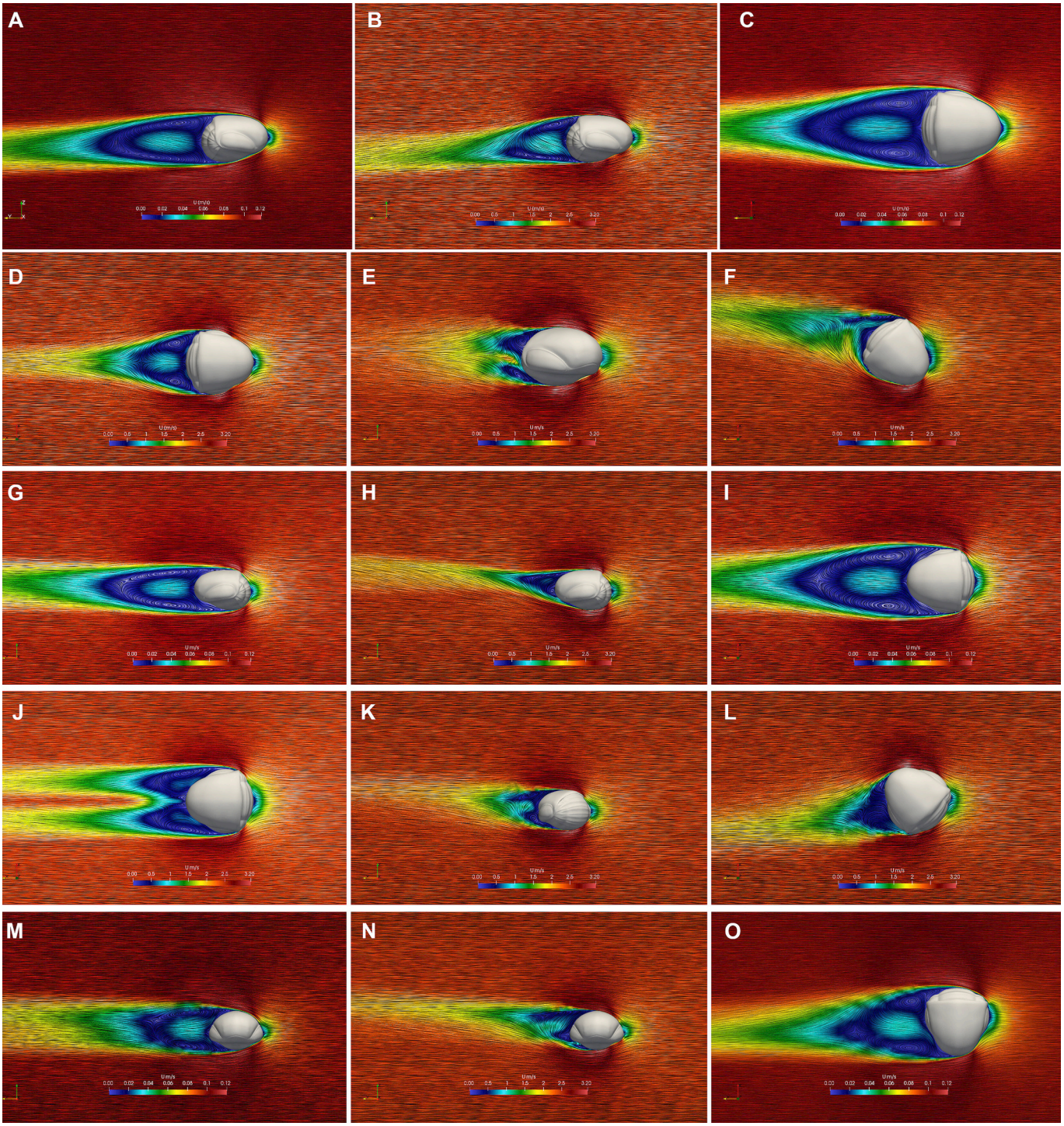

Fig. 6. Velocity field for CFD simulations in enrolled position.

the water via suction (Colin et al., 2020; Gemmell et al., 2015). Such swimming using suction thrust is very common in invertebrates using a metachronal swimming (Colin et al., 2020), which supports this sort of swimming for *Microparia*. In addition, when *Microparia speciosa* is swimming using a favorable current (parallel or obliquely to the current), different vortices are developed, comparable to those used by fish to save energy (Liao et al., 2003; Takagi, 2015). The biramous appendages of *Microparia speciosa* were likely the propulsion agents for swimming. The low velocity of the fluid below the *Microparia speciosa* body is a condition needed for paddle propulsion (Ford et al., 2019; Granzier-Nakajima et al., 2020; Takagi, 2015). Yet, appendages in asaphoids are known only in two taxa (Gutiérrez-Marco et al., 2017; Zeng et al., 2017) and unfortunately the no appendages of pelagic trilobite are known. We have to assume that *Microparia speciosa* used the exopod as a paddle for propulsion. Besides, negative pressure is needed in swimming arthropods to generate downward momentum in order to maintain their position in the water column (Ford et al., 2019). *Microparia speciosa* shows a very neutral pressure, but in living arthropods this negative pressure is increased by the metachronal paddling used to maintain their position in the water column during quiet (i.e., hovering) and fast forward swimming (Ford et al., 2019; Granzier-Nakajima et al., 2020). Here two different mechanisms could be used for *Microparia*

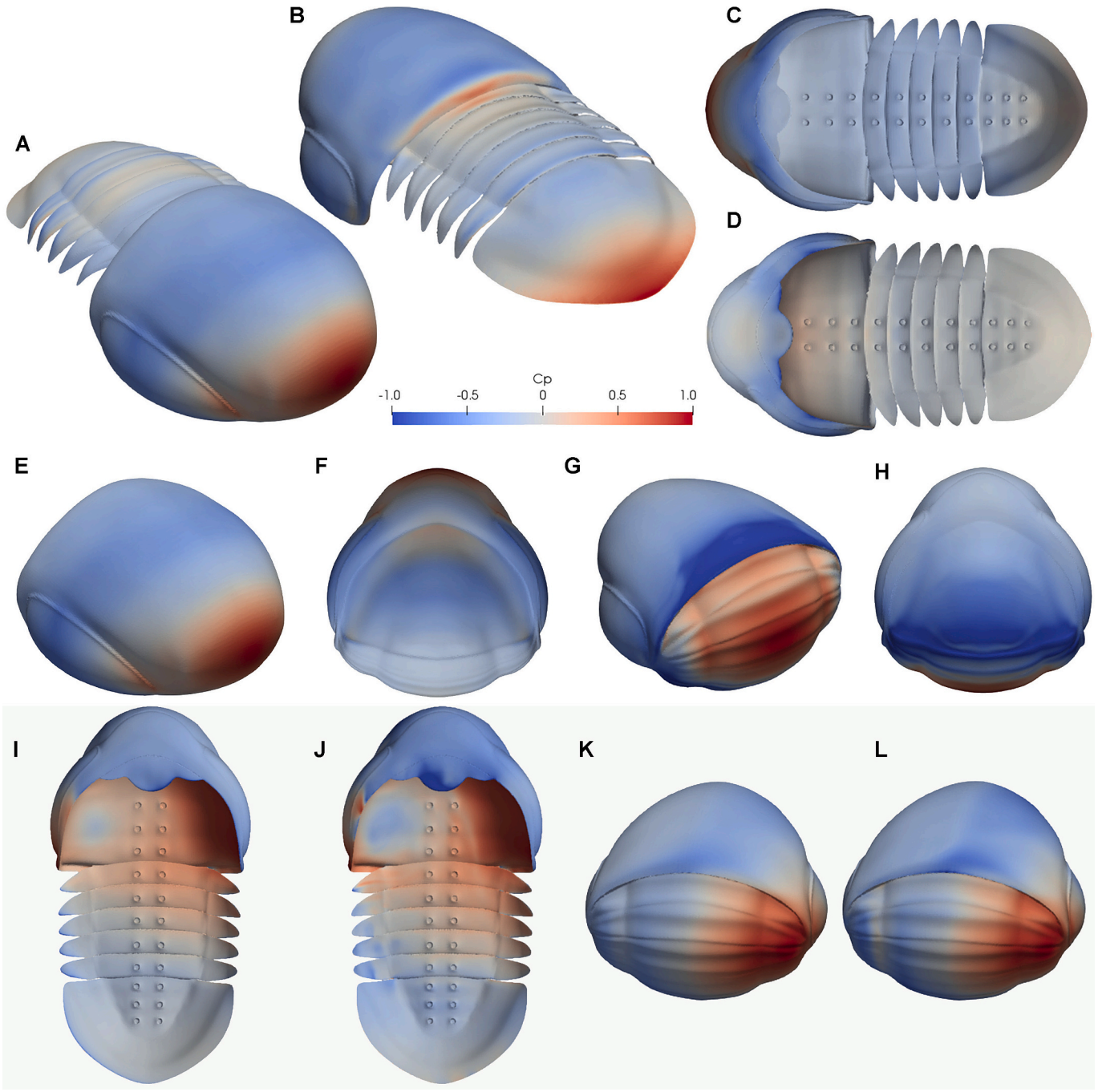

Fig. 7. Pressure coefficient (Cp) for CFD simulations in prone and enrolled positions.

speciosa to swim: i) synchronous recovery stroke, moving all appendages at once and ii) metachronal recovery stroke (Van Duren and Videler, 2003). These two mechanisms dependent on behavior, if *Microparia speciosa* wanted to escape from a predator it could use synchronous recovery stroke to reduce the drag and increase the speed in the water column (Van Duren and Videler, 2003). Thus, according to our results and given that the contemporaneous benthic trilobites used metachronal for locomotion on the seafloor (Osgood, 1970) and if living biramous and uniramous pelagic arthropods are metachronal swimmers (Alexander, 1988; Ford et al., 2019; Granzier-Nakajima et al., 2020), we can state that *Microparia speciosa* also was likely to have been a metachronal swimmer (see movie S7 in the supplementary material). Furthermore, metachronal swimming patterns prevent conflict with neighbouring appendages, since legs working as a member of a metachronal system move water more efficiently than an isolated limb (Lowndes, 1935; Marshall, 1973; Van Duren and Videler, 2003). The lift coefficient in *Microparia speciosa* is rather low in all prone simulation increasing with higher flow velocities. This improves stabilization in maintaining a vertical position when *Microparia speciosa* was swimming steadily. Metachronal swimming could also generate lift to improve swimming as in living pelagic arthropods especially during low Reynolds number regimes (Murphy et al., 2013).

The negative pressure measure on the pygidial side of enrolled simulations and the low lift coefficient recorded in all simulations represent the suitable conditions for hovering (Lauder, 2015; Murphy et al., 2013; Takagi, 2015) (see movie S8 in the supplementary material). In addition, the wake observed in the flow velocities field is always very symmetrical suggesting a steady scenario for hovering. This

represents a new function for enrolment in trilobites, not only for protection against predators but also as a hydrodynamic tool to maintain stability within the water column. Thus, *Microparia speciosa* takes advantage of a "plesiomorphic" behavior (i.e., enrolment) to occupy a special ecological niche in the pelagic or mesopelagic habitat.

4.2. Feeding strategy and nekton life habits during the Ordovician radiations

Feeding currents are given under viscous forces (i.e., low Reynolds number) assisted by metachronal swimming (Ford et al., 2019; Granzier-Nakajima et al., 2020; Jiang et al., 1999; Koehl and Strickler, 1981; Murphy et al., 2013; Takagi, 2015). Therefore, the CFD results suggest a steady scenario for feeding in *Microparia*. The flow velocities fields for the prone CFD simulations, especially the current and the kind of swimming (hovering and metachronal propulsion) produces swirls and eddies below and on either side of the moving *Microparia speciosa* and it is these eddies which are used in filter-feeding (Fig. 5A, D, see movies S1-S6 in the supplementary material). This supports the idea that pelagic trilobites fed on planktons in the water column (Cannon, 1928). Cannon (1928) already showed how vortices below the body of today's copepods were used for feeding in currents during hovering. The lack of legs in our simulations is not an obstacle since metachronal propulsion in pelagic and mesopelagic arthropods is given at low and intermediate Reynolds numbers (Granzier-Nakajima et al., 2020; Jiang et al., 1999).

These results show an important ecological novelty during the Ordovician radiations and support the idea developed by Whalen and Briggs (2018) of a progressive adoption of nektonic habits in the Palaeozoic seas. *Microparia speciosa* moved using currents to hover; their hydrodynamic profile was likely more important to produce proper vortices for feeding rather than swimming. Low drag coefficients in benthic or nektobenthic trilobites like *Hypodicranotus striatus* and *Placoparia cambriensis* probably exploited their geometry to induce water flow through the anterior cephalic arch along the food chamber taking food particles directly to the position of the mouth beneath the hypostome. *Microparia speciosa* represents the next step of progressive evolution in trilobites from living on the seafloor to a life in the open sea far from the benthos, evolving a new pelagic ecological niche during the Ordovician radiations. This progressive evolution to pelagic niche is also mirrored by early developmental trilobite stages (Laibl et al., 2023). However, this lifestyle in trilobites disappeared at the end of the Ordovician (Whalen and Briggs, 2018) may be linked to the better adaptation for swimming and predation in the water column shown by cephalopods and fishes.

Supplementary data to this article can be found online at https://doi.org/10.1016/j.palaeo.2023.111691.

Declaration of Competing Interest

The authors declare the following financial interests/personal relationships which may be considered as potential competing interests: Jorge Esteve reports financial support and equipment, drugs, or supplies were provided by Ministry of Science Technology and Innovations.

Data availability

All data needed to evaluate the conclusions in the paper are present in the paper and/or the Supplementary Materials.

Acknowledgements

We are grateful to Richard Fortey (NHM, London) for his comments and suggestions of the early version of this paper. We thank Zuzana Heřmanová (National Museum, Prague) for her assistance with X-ray microtomography, and her kind access to collections. Lukas Laibl (Prague) and Franco Tortello (La Plata) reviewed this manuscript. We thank to Thomas Servais (Lille) for his comments. This is a contribution to the project "Environmental and biogeochemical perturbations associated with the Cambrian Explosion and the Ordovician Biodiversification in West Gondwana and Baltica" (Grant no PID2021-125585NB-I00) supported by the Spanish Ministry of Science and Innovation. M.L.C. is supported by the European Union's Horizon 2020 research and innovation programme under the Marie Skłodowska-Curie grant agreement No. 945413 (Martí-Franquès COFUND Fellowship). This is a contribution to IGCP project 735 'Rocks and the Rise of Ordovician Life: Filling knowledge gaps in the Early Palaeozoic Biodiversification'.

Appendix A. Supplementary materials

Supplementary materials can be found online at https://drive.google.com/drive/folders/10ALuZxtvvC55M4EYGj79iuB3tIb-LF_m?usp=drive_link

References

Alexander, D.E., 1988. Kinematics of Swimming in two Species of Idotea (ISOPODA: Valvifera). J. Exp. Biol. 138, 37–49. https://doi.org/10.1242/jeb.138.1.37.

Cannon, H.G., 1928. On the Feeding Mechanism of the Copepods, Calanus Finmarchicus and Diaptomus Gracilis. J. Exp. Biol. 6, 131–144. https://doi.org/10.1242/jeb.6.2.131.

Colin, S.P., Costello, J.H., Sutherland, K.R., Gemmell, B.J., Dabiri, J.O., Du Clos, K.T., 2020. The role of suction thrust in the metachronal paddles of swimming invertebrates. Sci. Rep. 10, 17790. https://doi.org/10.1038/s41598-020-74745-y.

Dittrich, B., 1987. Postembryonic development of the parasitic amphipod Hyperia galba. Helgoläander Meeresuntersuchungen 41, 217–232. https://doi.org/10.1007/BF02364701.

Esteve, J., Hughes, N.C., Zamora, S., 2011. Purujosa trilobite assemblage and the evolution of trilobite enrollment. Geology 39, 575–578. https://doi.org/10.1130/G31985.1.

Esteve, J., Gutiérrz-Marxo, J.C., Rubio, P., Rábano, I., 2018. Evolution of trilobite enrolment during the Great Ordovician Biodiversification Event: insights from kinematic modelling. Lethaia 51, 207–217. https://doi.org/10.1111/let.12242.

Esteve, J., López, M., Ramírez, C.G., Gómez, I., 2021. Fluid dynamic simulation suggests hopping locomotion in the Ordovician trilobite Placoparia. J. Theor. Biol. 531 https://doi.org/10.1016/j.jtbi.2021.110916.

Esteve, J., Sundberg, F.A., Zamora, S., Gozalo, R., 2012. A new Alokistocaridae Resser, 1939 (Trilobita) from the middle Cambrian of Spain. Geobios. https://doi.org/10.1016/j.geobios.2011.10.003.

Ford, M.P., Lai, H.K., Samaee, M., Santhanakrishnan, A., 2019. Hydrodynamics of metachronal paddling: Effects of varying Reynolds number and phase lag. R. Soc. Open Sci. 6, 191387 https://doi.org/10.1098/rsos.191387.

Fortey, R.A., 1985. Pelagic trilobites as an example of deducing the life habits of extinct arthropods. Trans. R. Soc. Edinb. Earth Sci. 76, 219–230. https://doi.org/10.1017/S0263593300010452.

Fortey, R.A., Owens, R.M., 1999. Feeding habits in trilobites. Palaeontology 42, 429–465. https://doi.org/10.1111/1475-4983.00080.

Gemmell, B.J., Colin, S.P., Costello, J.H., Dabiri, J.O., 2015. Suction-based propulsion as a basis for efficient animal swimming. Nat. Commun. 6 https://doi.org/10.1038/ncomms9790.

Granzier-Nakajima, S., Guy, R.D., Zhang-Molina, C., 2020. A numerical study of metachronal propulsion at low to intermediate Reynolds numbers. Fluids 5, 1–15. https://doi.org/10.3390/fluids5020086.

Gutiérrez-Marco, J.C., García-Bellido, D.C., Rábano, I., Sá, A.A., 2017. Digestive and appendicular soft-parts, with behavioural implications, in a large Ordovician trilobite from the Fezouata Lagerstätte, Morocco. Sci. Rep. 7, 39728. https://doi.org/10.1038/srep39728.

Harper, D.A.T., Cascales-Miñana, B., Servais, T., 2020. Early Palaeozoic diversifications and extinctions in the marine biosphere: a continuum of change. Geol. Mag. 157, 5–21. https://doi.org/10.1017/S0016756819001298.

Harper, D.A.T., Cascales-Miñana, B., Kroeck, D.M., Servais, T., 2021. The palaeogeographic impact on the biodiversity of marine faunas during the Ordovician radiations. Glob. Planet. Chang. 204, 103665 https://doi.org/10.1016/j.gloplacha.2021.103665.

Haug, C., Haug, J.T., 2014. Defensive enrolment in mantis shrimp larvae (Malacostraca: Stomatopoda). Contrib. Zool. 83, 185–194. https://doi.org/10.1163/18759866-08303003.

Hessler, R.R., 1985. Swimming in Crustacea. Trans. R. Soc. Edinb. Earth Sci. 76, 115–122. https://doi.org/10.1017/S0263593300010385.

Hopkins, M.J., 2014. The environmental structure of trilobite morphological disparity. Paleobiology 40, 352–373. https://doi.org/10.1666/13049.

Jacklyn, P.M., Ritz, D.A., 1986. Hydrodynamics of swimming in scyllarid lobsters. J. Exp. Mar. Biol. Ecol. 101, 85–99. https://doi.org/10.1016/0022-0981(86)90043-2.

Jeffs, A.G., Holland, R.C., 2000. Swimming behaviour of the puerulus of the spiny lobster, Jasus edwardsii (Hutton, 1875) (Decapoda, Palinuridae). Crustaceana. https://doi.org/10.1163/156854000504859.

Jiang, H., Meneveau, C., Osborn, T.R., 1999. Numerical study of the feeding current around a copepod. J. Plankton Res. 21, 1391–1421. https://doi.org/10.1093/plankt/21.8.1391.

Koehl, M.A.R., Strickler, J.R., 1981. Copepod feeding currents: food capture at low Reynolds number. Limnol. Oceanogr. 26, 1062–1073. https://doi.org/10.4319/lo.1981.26.6.1062.

Laibl, L., Saleh, F., Pérez-Peris, F., 2023. Drifting with trilobites: The invasion of early post-embryonic trilobite stages to the pelagic realm. Palaeogeogr. Palaeoclimatol. Palaeoecol. 613, 111403.

Lauder, G.V., 2015. Fish locomotion: recent advances and new directions. Annu. Rev. Mar. Sci. 7 https://doi.org/10.1146/annurev-marine-010814-015614.

Lerosey-Aubril, R., Angiolini, L., 2009. Permian trilobites from Antalya Province, Turkey, and enrollment in late Palaeozoic trilobites. Turk. J. Earth Sci. 18, 427–448. https://doi.org/10.3906/yer-0801-5.

Lewis, A.G., Allen, S.E., Martens, G., 2006. Rapid swimming and the median intersomitic ridge in calanoid copepods. Crustaceana 79, 501–511. https://doi.org/10.1163/156854006777554794.

Liao, J.C., Beal, D.N., Lauder, G.V., Triantafyllou, M.S., 2003. Fish exploiting vortices decrease muscle activity. Science 302, 1566–1569. https://doi.org/10.1126/science.1088295.

Lochhead, J.H., 1977. Unsolved problems of interest in the locomotion of crustacea. In: Pedley, T.J. (Ed.), Scale Effects in Animal Locomotion. Academic Press, pp. 257–268.

Lochhead, J.H., 1961. Locomotion. In: Waterman, T.H. (Ed.), Physiology of Crustacea Vol. II. New York.

Lowndes, A.G., 1935. The Swimming and Feeding of certain Calanoid Copepods. In: Proceedings of the Zoological Society of London 105. https://doi.org/10.1111/j.1096-3642.1935.tb01688.x.

Lumpkin, R., Johnson, G.C., 2013. Global Ocean surface velocities from drifters: mean, variance, El Niño-Southern Oscillation response, and seasonal cycle. J.Geophys.Res. Oceans 2992–3006. https://doi.org/10.1002/jgrc.20210.

Marek, L., 1961. The trilobite Family Cyclopygidae Raymond in the Ordovician of Bohemia. Rozpr. Ustred. Ust. 28, 1–81.

Marshall, S.M., 1973. Respiration and feeding in copepods. Adv. Mar. Biol. 11, 57–120. https://doi.org/10.1016/S0065-2881(08)60268-0.

Murphy, D.W., Webster, D.R., Yen, J., 2013. The hydrodynamics of hovering in Antarctic krill. Limnol.Oceanogr.Fluids Environ. 3, 240–255. https://doi.org/10.1215/21573689-2401713.

Ortega-Hernández, J., Esteve, J., Butterfield, N.J., 2013. Humble origins for a successful strategy: complete enrolment in early Cambrian olenellid trilobites. Biol. Lett. https://doi.org/10.1098/rsbl.2013.0679.

Osgood Jr., R.G., 1970. Trace fossils of the Cincinatti area. Palaeontogr. Am. 6, 1–146.

Paffenhöfer, G.A., Strickler, J.R., Alcaraz, M., 1982. Suspension-feeding by herbivorous calanoid copepods: a cinematographic study. Mar. Biol. 67 https://doi.org/10.1007/BF00401285.

Servais, T., Cascales-Miñana, B., Harper, D.A.T., Lefebvre, B., Munnecke, A., Wang, W.H., Zhang, Y.D., 2023. No (Cambrian) explosion and no (Ordovician) event: a single long-term radiation in the early Palaeozoic. Palaeogeogr. Palaeoclimatol. Palaeoecol. 111592 https://doi.org/10.1016/j.palaeo.2023.111592.

Shiino, Y., Kuwazuru, O., Suzuki, Y., Ono, S., 2012. Swimming capability of the remopleuridid trilobite Hypodicranotus striatus: hydrodynamic functions of the exoskeleton and the long, forked hypostome. J. Theor. Biol. 7, 29–38. https://doi.org/10.1016/j.jtbi.2012.01.012.

Shiino, Y., Kuwazuru, O., Suzuki, Y., Ono, S., Masuda, C., 2014. Pelagic or benthic? Mode of life of the remopleuridid trilobite Hypodicranotus striatulus. Bull. Geosci. 89, 207–218. https://doi.org/10.3140/bull.geosci.1409.

Stigall, A.L., Edwards, C.T., Freeman, R.L., Rasmussen, C.M.Ø., 2019. Coordinated biotic and abiotic change during the Great Ordovician Biodiversification Event: Darriwilian assembly of early Paleozoic building blocks. Palaeogeogr. Palaeoclimatol. Palaeoecol. 530, 249–270. https://doi.org/10.1016/j.palaeo.2019.05.034.

Strickler, J.R., 1982. Calanoid copepods, feeding currents, and the role of gravity. Science 218, 158–160. https://doi.org/10.1126/science.218.4568.158.

Strickler, J.R., 1977. Observation of swimming performances of planktonic copepods. Limnol. Oceanogr. https://doi.org/10.4319/lo.1977.22.1.0165.

Takagi, D., 2015. Swimming with stiff legs at low Reynolds number. Phys. Rev. E Stat. Nonlinear Soft Matter Phys. 92, 023020 https://doi.org/10.1103/PhysRevE.92.023020.

Van Duren, L.A., Videler, J.J., 2003. Escape from viscosity: the kinematics and hydrodynamics of copepod foraging and escape swimming. J. Exp. Biol. 206, 269–279. https://doi.org/10.1242/jeb.00079.

Veizer, J., Buhl, D., Diener, A., Ebneth, S., Podlaha, O.G., Bruckschen, P., Jasper, T., Korte, C., Schaaf, M., Ala, D., Azmy, K., 1997. Strontium isotope stratigraphy: potential resolution and event correlation. Palaeogeogr. Palaeoclimatol. Palaeoecol. 132, 65–77. https://doi.org/10.1016/S0031-0182(97)00054-0.

Veizer, J., Prokoph, A., 2015. Temperatures and oxygen isotopic composition of Phanerozoic oceans. Earth Sci. Rev. https://doi.org/10.1016/j.earscirev.2015.03.008.

Whalen, C.D., Briggs, D.E.G., 2018. The Palaeozoic colonization of the water column and the rise of global nekton. Proc. R. Soc. B Biol. Sci. 285, 20180883. https://doi.org/10.1098/rspb.2018.0883.

Zeng, H., Zhao, F., Yin, Z., Zhu, M., 2017. Appendages of an early Cambrian metadoxidid trilobite from Yunnan, SW China support mandibulate affinities of trilobites and artiopods. Geol. Mag. 1–23 https://doi.org/10.1017/S0016756817000279.